

9. North, K., Joy, P., Yuille, D., Cocks, N. & Hutchins, P. Cognitive function and academic performance in children with neurofibromatosis type 1. *Dev. Med. Child Neurol.* **37**, 427–436 (1995).

10. North, K. *et al.* Specific learning disability in children with neurofibromatosis type 1: significance of MRI abnormalities. *Neurology* **44**, 878–883 (1994).

11. Silva, A. J. *et al.* A mouse model for the learning and memory deficits associated with neurofibromatosis type 1. *Nature Genet.* **15**, 281–284 (1997).

12. The, I. *et al.* Rescue of a *Drosophila* *NF1* mutant phenotype by protein kinase A. *Science* **276**, 791–794 (1997).

13. Guo, H. F., The, I., Hannan, F., Bernards, A. & Zhong, Y. Requirement of *Drosophila* *NF1* for activation of adenylyl cyclase by PACAP38-like neuropeptide. *Science* **276**, 795–798 (1997).

14. Livingstone, M. S., Sziber, P. P. & Quinn, W. G. Loss of calcium/calmodulin responsiveness in adenylyl cyclase of *rutabaga*, a *Drosophila* learning mutant. *Cell* **37**, 205–215 (1984).

15. Han, P.-L., Levin, L. R., Reed, R. R. & Davis, R. L. Preferential expression of the *Drosophila* *rutabaga* gene in mushroom bodies, neural centers for learning in insects. *Neuron* **9**, 619–627 (1992).

16. Tully, T. & Quinn, W. G. Classical conditioning and retention in normal and mutant *Drosophila melanogaster*. *J. Comp. Physiol. A Sens. Neural. Behav. Physiol.* **157**, 263–277 (1985).

17. de Belle, J. S. & Heisenberg, M. Associative odor learning in *Drosophila* abolished by chemical ablation of mushroom bodies. *Science* **263**, 692–695 (1994).

18. Connolly, J. B. *et al.* Associative learning disrupted by impaired Gs signaling in *Drosophila* mushroom bodies. *Science* **274**, 2104–2106 (1996).

19. Grotewiel, M. S., Beck, C. D., Wu, K. H., Zhu, X. R. & Davis, R. L. Integrin-mediated short-term memory in *Drosophila*. *Nature* **391**, 455–460 (1998).

20. Dura, J.-M., Preat, T. & Tully, T. Identification of *linotte*, a new gene affecting learning and memory in *Drosophila melanogaster*. *J. Neurogenetics* **9**, 1–14 (1993).

21. Yin, J. C. P. *et al.* Induction of a dominant negative CREB transgene specifically blocks long-term memory in *Drosophila*. *Cell* **79**, 49–58 (1994).

22. Levin, L. R. *et al.* The *Drosophila* learning and memory gene *rutabaga* encodes a Ca²⁺/calmodulin-responsive adenylyl cyclase. *Cell* **68**, 479–489 (1992).

23. Byers, D., Davis, R. L. & Kiger, J. A. Defect in cyclic-AMP phosphodiesterase due to the dunce mutation of learning in *Drosophila melanogaster*. *Nature* **289**, 79–81 (1981).

24. Chen, C. N., Denome, S. & Davis, R. L. Molecular analysis of cDNA clones and the corresponding genomic coding region of the *Drosophila* *dunce*⁺ locus, the structure gene for cAMP phosphodiesterase. *Proc. Natl Acad. Sci. USA* **86**, 3599–3603 (1986).

25. Jiang, J. & Struhl, G. Protein kinase A and *hedgehog* signaling in *Drosophila* limb development. *Cell* **80**, 563–572 (1995).

26. Mitts, M. R., Bradshaw-Rouse, J. & Heideman, W. Interactions between adenylyl cyclase and the yeast GTPase-activating protein IRA1. *Mol. Cell. Biol.* **11**, 4591–4598 (1991).

27. Livingstone, M. S. Genetic dissection of *Drosophila* adenylyl cyclase. *Proc. Natl Acad. Sci. USA* **82**, 5992–5996 (1985).

28. Bers, D. M., Patton, C. W. & Nuccitelli, R. A practical guide to the preparation of Ca²⁺ buffers. *Methods. Cell. Biol.* **40**, 3–29 (1994).

29. O'Connell, P. & Rosbash, M. Sequence, structure and codon preference of the *Drosophila* ribosomal protein 49 gene. *Nucleic Acids Res.* **12**, 5495–5513 (1984).

Acknowledgements

We thank T. Tully for help with behavioural assays, R. Davis for extensive comments on the manuscript, and A. Bernards for providing the fly stocks. This work was supported by a Pew Scholarship, grants from NIH, grants from Texas Neurofibromatosis foundation, NF Inc. Mass Bay Aere and Illinois NF Inc., Perkin fund, and donations from M. L. Rankowitz and S. H. Heffron to Y.Z., and by a National Neurofibromatosis Foundation Young Investigator Award to F.H.

Three distinct and sequential steps in the release of sodium ions by the Na⁺/K⁺-ATPase

Miguel Holmgren*, Jonathan Wagg*, Francisco Bezanilla*, Robert F. Rakowski*, Paul De Weer* & David C. Gadsby*

The Marine Biological Laboratory, Woods Hole, Massachusetts 02543, USA

The Na⁺/K⁺ pump, a P-type ion-motive ATPase, exports three sodium ions and then imports two potassium ions in each transport cycle. Ions on one side of the membrane bind to sites within the protein and become temporarily occluded (trapped within the protein) before being released to the other side^{1,2}, but

* Present addresses: Department of Neurobiology, Harvard Medical School, Boston, Massachusetts 02115, USA (M.H.); rSafe Inc, 369 Pine St, San Francisco, California 94104, USA (J.W.); Department of Physiology, UCLA School of Medicine, Los Angeles, California 90095, USA (F.B.); Department of Physiology and Biophysics, FUHS/Chicago Medical School, North Chicago, Illinois 60064, USA (R.F.R.); Department of Physiology, University of Pennsylvania School of Medicine, Philadelphia, Pennsylvania 19104, USA (P.D.); Laboratory of Cardiac Membrane Physiology, The Rockefeller University, New York, New York 10021, USA (D.C.G.).

details of these occlusion and de-occlusion transitions remain obscure for all P-type ATPases. If it is deprived of potassium ions, the Na⁺/K⁺ pump is restricted to sodium translocation steps³, at least one involving charge movement through the membrane's electric field^{4,5}. Changes in membrane potential alter the rate of such electrogenic reactions and so shift the distribution of enzyme conformations. Here we use high-speed voltage jumps to initiate this redistribution and show that the resulting pre-steady-state charge movements relax in three identifiable phases, apparently reflecting de-occlusion and release of the three sodium ions. Reciprocal relationships among the sizes of these three charge components show that the three sodium ions are de-occluded and released to the extracellular solution one at a time, in a strict order.

The main electrical signals generated during Na⁺/K⁺ pumping result from Na⁺ traversing part of the membrane's electric field in an access channel that connects Na⁺-binding sites to the extracellular medium^{6–9}. To investigate de-occlusion and release of the three transported Na⁺ ions, we measured pump-mediated charge translocation in voltage-clamped, internally dialysed squid giant axons, using solutions designed to limit Na⁺/K⁺ pumps to phosphorylated conformations with Na⁺-binding sites either occupied and buried or open to the external solution: (Na₃)E₁-P ↔ P-E₂-Na₃ ↔ P-E₂ (Fig. 1, dotted box). Pump-mediated charge was assayed as the component of membrane current that was sensitive to dihydrodigi-toxigenin (H₂DTG), a specific Na⁺/K⁺-pump inhibitor¹⁰ (Fig. 2a (2–3)). With 100 mM external Na⁺ ([Na]_o), the change in pump current induced by a voltage jump (20-ms step from 0 mV to –90 mV; current displayed at 50 μs per point in Fig. 2a) comprised fast (the first ~10 points) and slow (τ ≈ 4 ms) components, and relaxed to near zero. As negative internal potentials electrostatically favour the approach of external Na⁺ to their binding sites within the pump, we interpret the fast component (see ref. 8) as reflecting rapid electrogenic binding of Na_o⁺ to vacant sites (P-E₂) to satisfy the new P-E₂ ↔ P-E₂-Na₃ distribution demanded by the new membrane potential, –90 mV. The resulting increased abundance of pumps in the P-E₂-Na₃ state drives the slower (comparatively electroneutral; see below) occlusion reaction (P-E₂-Na₃ ↔ (Na₃)E₁-P), which is tracked by further electrogenic binding of Na_o⁺ to P-E₂, now rate limited by the slow conformational change and hence appearing as slow charge movement (see, for example, refs 7, 11). We found no recruitment of additional slow charge (Q_s; Fig. 2b, left) at extreme potentials, in accord with the expectation that, in the steady state, pumps in the P-E₂ conformation should be

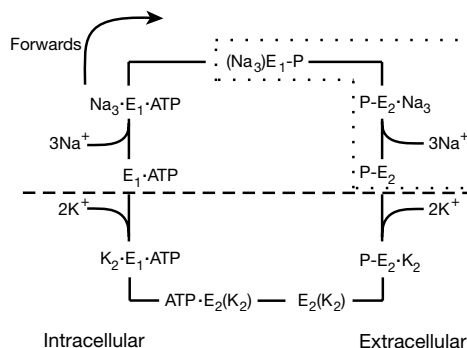


Figure 1 Simplified Post-Albers transport cycle emphasizing two principal Na⁺/K⁺ pump conformations: E₁ with ion-binding sites facing the cytoplasm, and E₂ with ion-binding sites open to the extracellular solution. Phosphorylation of E₁ by ATP occludes three Na⁺, which are released to the external medium after the conformational change to E₂, whereupon two K⁺ bind, eliciting dephosphorylation and K⁺ occlusion. ATP binding favours transition back to E₁, prompting K⁺ release to the cytoplasm and binding of three Na⁺, completing the cycle. The dashed (horizontal) line separates Na⁺- and K⁺-translocation pathways; the dotted box encloses states isolated experimentally to yield the charge movements examined.

scarce at very negative potentials but maximally abundant at very positive potentials. Also as expected, the positive and negative potentials at which slow charge recruitment effectively ceased depended on $[Na]_o$ (Fig. 2b, left): at lower $[Na]_o$ less positive potentials can fully unload Na^+ -binding sites, and at higher $[Na]_o$ less negative potentials are required for Na^+ to fill all P-E₂ sites.

The relaxation rate (k) of the slow component reached a minimum ($\sim 100\text{ s}^{-1}$) at positive potentials, but became faster at negative potentials, and tended towards saturation (at $\sim 1,400\text{ s}^{-1}$) at large

negative voltages (Fig. 2b, right). This may indicate that, ultimately, regardless of $[Na]_o$, the reactions limiting the rates of the slow charge translocation in both the forwards (de-occlusion: extreme positive potentials) and backwards (occlusion: extreme negative potentials) directions are nearly electroneutral^{7,8,12}. Between these extremes the slow relaxation rate varies with $[Na]_o$ and voltage, reflecting the filling of Na^+ -binding sites¹¹. Fitting these slow rates (curves, Fig. 2b, right) to the simple three-state scheme (Fig. 1, box) gave an estimate for the fraction (λ) of the membrane's electric field dropped along the access channel of 71% similar to our previous estimate (69%) from analysis of the voltage dependence of $^{22}Na^+$ efflux mediated by Na_i/Na_o exchange under similar conditions⁷.

We tested whether the reactions underlying the fast and slow components of pump charge movement occur in sequence, as implied above, by making the membrane potential negative enough (-110 mV) for long enough (20 ms) for complete relaxation of the current in 400 mM $[Na]_o$ before stepping back to 0 mV. As anticipated, this conditioning step elicited a large fast component (reflecting Na^+ binding) followed by a slow relaxation (reflecting occlusion); but, although the jump back to 0 mV caused the return movement of a comparable amount of slow charge, the fast component preceding it was greatly reduced (Fig. 3a). Evidently, because the occlusion/de-occlusion reaction is strongly poised towards occlusion at -110 mV in high $[Na]_o$ (Fig. 2b, left), the prolonged sojourn at this potential drove most pumps to the occluded state, (Na_3)E₁-P, whence they could not immediately release Na^+ (to generate rapid charge movement) when the potential was returned to 0 mV. Positive voltage jumps also elicit fast and slow movements of pump-mediated charge (Fig. 3b), the fast component in this case reflecting migration of released Na^+ ions out through the access channel, and the slow component tracking the rate-limiting de-occlusion step. The prolonged positive potential should thus leave newly unloaded pumps available to bind Na^+ and, hence, to contribute to a slightly larger fast charge component upon the jump back to 0 mV (as observed, Fig. 3b). These findings with long conditioning voltage steps show that the reactions underlying the fast and slow charge movements are obliged to occur in sequence.

The simple scheme of Fig. 1 cannot, however, explain the comparable amounts of slow charge moved during and after long conditioning voltage jumps (for example, Figs 2a, 3a), particularly large negative jumps⁸. If the three Na^+ bind virtually instantaneously to P-E₂, as implied (Fig. 1), a sufficiently negative voltage jump should rapidly saturate available Na^+ -binding sites, causing a maximally large movement of fast-charge. But, if the

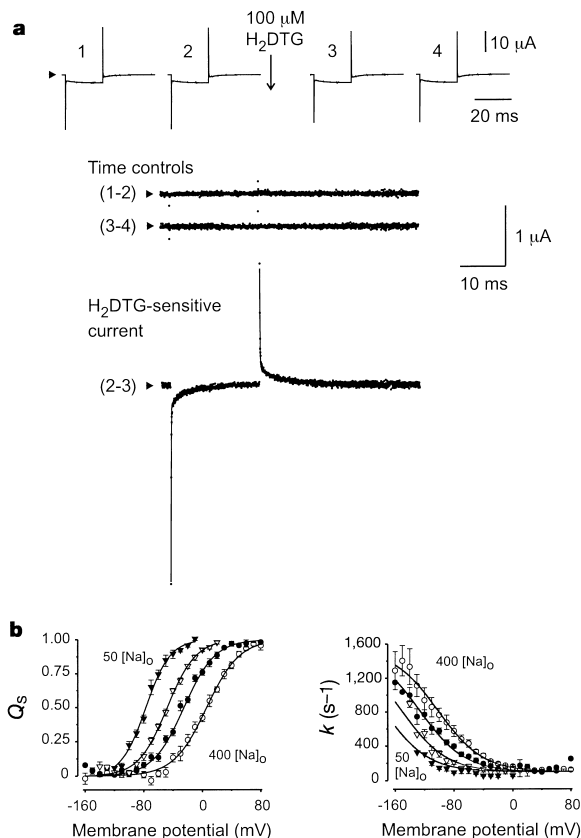


Figure 2 Charge movement during Na^+ translocation by the Na^+/K^+ pump. **a**, Determination of H_2DTG -sensitive (pump-mediated) current. Traces 1–4 show averages of 100 current responses to 20-ms voltage jumps, from 0 to -90 mV , applied at 4-min intervals to an axon exposed to 100 mM $[Na]_o$ without (1 and 2) or with (3 and 4) 100 μM H_2DTG . Difference currents (1–2) and (3–4) show stability with time; (2–3) shows pump-mediated current fitted with a two-exponential function (solid lines largely obscured by data points), yielding τ values of 0.06 ms and 4 ms at -90 mV (on), and 0.1 ms and 5 ms at 0 mV (off). Arrowheads mark zero current. Filter 5 kHz, sampling 20 kHz. **b**, Voltage dependence of slow component, elicited by 20–40-ms jumps from -40 mV at 400 (open circles), 200 (filled circles), 100 (open triangles) or 50 (filled triangles) mM $[Na]_o$. Left, normalized slow charge (Q_s); Boltzmann fits yield, at 400, 200, 100 or 50 mM $[Na]_o$, (equivalent valence) $z_q = 1.15 \pm 0.05$, 1.22 ± 0.04 , 1.32 ± 0.04 or 1.55 ± 0.09 , and (midpoint potential) $V_q = 6 \pm 1$, -25 ± 1 , -48 ± 1 or $-77 \pm 1\text{ mV}$. Right, relaxation rate constant (k); curves show simultaneous fit to modified Hill expression⁷:

$$k_{(v)} = k_f + \frac{k_b}{1 + \frac{K_{0.5}(0) \exp(\lambda VF/RT)}{[Na]_o^n}}$$

where k_f and k_b are voltage-independent forwards (de-occlusion) and backwards (occlusion) rate constants, $K_{0.5}(0)$ is half-activating $[Na]_o$ at 0 mV, n is the Hill coefficient and λ is the fraction of the electrical field dropped along the access channel. Overall best-fit values: $k_f = 97 \pm 12\text{ s}^{-1}$, $k_b = 1,444 \pm 367\text{ s}^{-1}$, $K_{0.5}(0) = 6.95 \pm 1.47\text{ M}$, $n = 1.17 \pm 0.1$ and $\lambda = 0.71 \pm 0.04$.

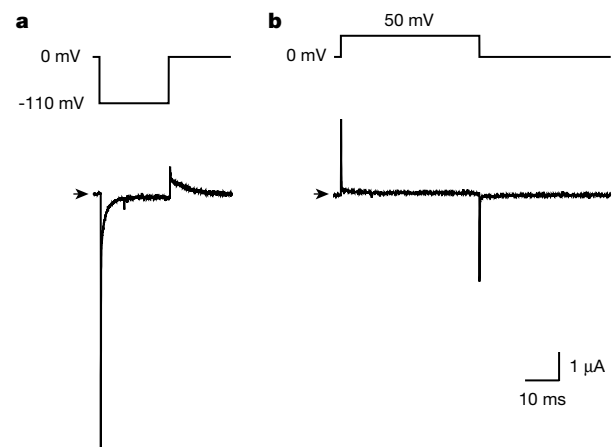


Figure 3 Non-conservation of fast charge between on and off voltage steps. **a**, H_2DTG -sensitive current at 400 mM $[Na]_o$ due to test step to -110 mV , with on-line subtraction of scaled linear capacitance current elicited by small steps from the steady potential, -110 mV . Filter 20 kHz, sampling 100 kHz. **b**, H_2DTG -sensitive current in the same axon with same conditions as **a**, but for step to $+50\text{ mV}$. Filter 20 kHz, sampling 50 kHz.

$P-E_2 \cdot Na_3 \leftrightarrow (Na_3)E_1-P$ occlusion reaction is intrinsically nearly electroneutral, as concluded, the subsequent slow conformational transition should engender only a negligible electrical signal, in contrast to the large movement of slow charge recorded (Fig. 3a). One proposal to account for such a discrepancy makes the access channel state a high-energy, short-lived conformation sandwiched between two occlusion/de-occlusion transitions⁸. This effectively limits the size of the rapid charge movement (because the access-channel state is rarely populated), but preserves a large slow component (because release and binding of external Na^+ must still proceed through the access channel). Our extension of the model (Fig. 4a) posits that the three Na^+ within $(Na_3)E_1-P$ are de-occluded and released one at a time (see also ref. 12). Two predictions of this new scheme are that the relaxation of pump current after a voltage jump should comprise more than two components, and that reciprocal relationships should exist between the magnitudes of those components.

To resolve additional components we increased the sampling rate to 2 MHz and used both briefer voltage steps and low $[Na]_o$ to avoid driving most pumps to the occluded state. Figure 4b shows the pump current elicited by a 500- μ s jump from 0 to -110 mV at 100 mM $[Na]_o$. Under these conditions the slow relaxation ($\tau \approx 3$ ms; Fig. 2b), appearing as an almost steady current at -100 mV, can move only $\sim 15\%$ of its charge during the 500- μ s pulse. Because it moves even more slowly at 0 mV ($\tau \approx 5$ ms; Fig. 2b), restoration of that small slow charge after the jump back to 0 mV is barely discernible as a small (practically time-independent) displacement above the zero-current line (Fig. 4b).

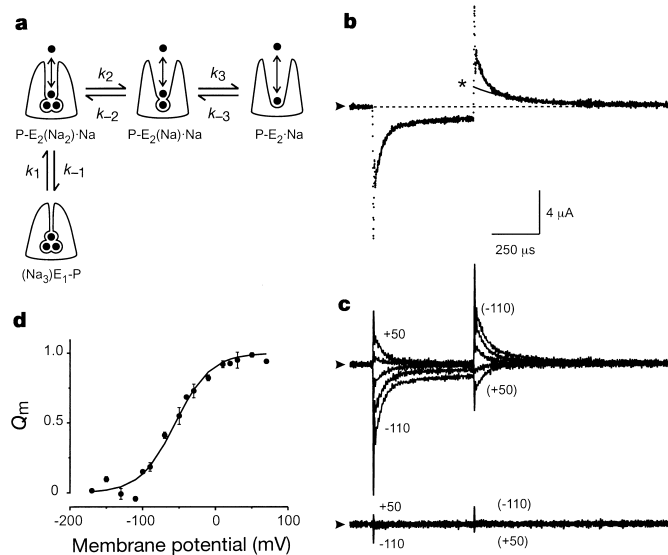


Figure 4 Faster sampling reveals medium-speed component. **a**, Model: predominant electrogenic events are assumed to be migration of released Na^+ (black balls) along access channels, narrow (high-field) for the first Na^+ but wide (low-field) for the next two Na^+ ; relatively electroneutral transitions (rate constants k_1/k_{-1} , k_2/k_{-2} and k_3/k_{-3}) de-occlude each Na^+ . **b**, Pump current elicited by 500- μ s step from 0 to -110 mV, at 100 mM $[Na]_o$; solid line (asterisk) shows 2-exponential fit (ignoring first 150 μ s) to off current; the medium-speed component, $\tau = 220 \mu$ s, was >20 -fold faster than the slow component, but ~ 10 -fold slower than the fast component(s) which relaxed in two phases (above fit line) with $\tau \approx 3 \mu$ s and $\approx 30 \mu$ s (closely matching two phases of capacitance current relaxation in that axon, and so reflecting the speed of membrane potential change). Filter 100 kHz, sampling 2 MHz. **c**, Superimposed pump currents for steps from 0 mV to +50, +10, -30, -70 and -110 mV at 100 mM $[Na]_o$; below, time controls show subtraction of records taken 4 min apart before adding H₂DTG. Filter 100 kHz, sampling 2 MHz. **d**, Voltage sensitivity of normalized medium-speed charge (Q_m ; mean, $n = 3$) at 50 mM $[Na]_o$, measured at 0 mV (as in **b**) after 500- μ s steps to indicated potentials; Boltzmann fit parameters, $z_q = 1.1 \pm 0.1$ and $V_q = -55 \pm 2$ mV.

The large-amplitude charge movements (two phases, mirroring the two phases of capacitance current decline; see Fig. 4b) that decay within the first $\sim 100 \mu$ s after both negative- and positive-going voltage steps correspond to the fast component already described (Figs 2a, 3). Then, however, a clear inflection in the current relaxation at 0 mV, $\sim 100 \mu$ s after its onset, reveals a subsequent additional, medium-speed component with a time constant of roughly 200 μ s (fitted curve; asterisk, Fig. 4b). The charge moved at 0 mV by this medium-speed component was small following jumps to positive potentials, but, like the slow component, it became prominent after pulses to potentials more negative than -70 mV (Fig. 4c), and its magnitude varied steeply with conditioning voltage (Fig. 4d).

If the underlying reactions are sequential (as proposed, Fig. 4a), each component (fast, medium-speed and slow) must develop at the expense of the preceding one. Figure 5a shows that the growth of the medium-speed component (assayed at 0 mV; fitted curves) with prolongation of the preceding -100-mV conditioning pulse from 200 to 800 μ s was accompanied by a decrease in the amplitude of the fast component. This growth of medium-speed charge (Q_m) with conditioning pulse duration was more rapid at 400 mM than at 100 mM $[Na]_o$ (Fig. 5b), occurring in both cases with a time course approximating the relaxation of the medium-speed component at -100 mV at the same $[Na]_o$. However, further prolongation of the conditioning pulse reduced the magnitude of the subsequent Q_m , with time constants similar to those measured directly for relaxation of the slow charge component at -100 mV and at the appropriate $[Na]_o$ (Fig. 2b). Together, these results support our model (Fig. 4a) by establishing that the medium-speed component grows at the expense of the fast component, but then wanes as it populates the enzyme conformations that generate the slow component.

We have shown here that the charge movements accompanying release of three Na^+ ions by the pump are rate limited by three

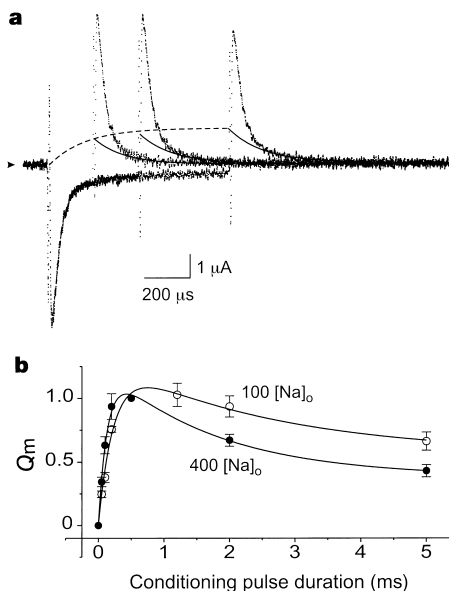


Figure 5 Sequential reactions underlie the three charge components. **a**, Conditioning pulse duration (200, 400 and 800- μ s steps from 0 to -100 mV at 50 mM $[Na]_o$) influences relative sizes of subsequent fast and medium-speed components: solid lines represent 2-exponential fits extrapolated to the off voltage jump; for all three traces, medium-speed $\tau = 140 \mu$ s. For illustration, an exponential curve (τ also 140 μ s) has been drawn through the extrapolated initial amplitudes. Filter 100 kHz, sampling 2 MHz. **b**, Normalized medium-speed charge (Q_m) moved at 0 mV after steps to -100 mV of indicated duration, at 100 mM (open circles) and 400 mM (filled circles) $[Na]_o$; curves are fits to difference of 2 exponentials, yielding τ values of 0.13 ± 0.01 and 1.74 ± 0.45 ms at 400 mM $[Na]_o$, whereas at 100 mM $[Na]_o$ τ values are 0.23 ± 0.01 and 2.6 ms (the latter constrained as the mean τ for the slow component at -100 mV and 100 mM $[Na]_o$, from Fig. 2b, right).

separate, sequential reactions, each of which probably opens a binding site to permit one Na⁺ to escape. Each charge component has well defined characteristics. The slowest appears to reflect strongly electrogenic (equivalent valence, $z \approx 1$; Fig. 2b) release of the first Na⁺, through $\sim 70\%$ of the membrane field, in a reaction that is rate limited by the slow (~ 100 to $1,400\text{ s}^{-1}$) major $E_1\text{-P} \leftrightarrow \text{P-E}_2$ conformational change, which itself seems relatively electroneutral; this slow component shows low sensitivity to $[\text{Na}]_o$ (Fig. 2b) but has strongly temperature-sensitive rates⁵, revealing an enthalpic activation energy of $\sim 80\text{ kJ mol}^{-1}$ ($10\text{--}20\text{ }^\circ\text{C}$; not shown; see ref. 13). Like the slow component, the medium-speed ($\sim 6,000$ to $20,000\text{ s}^{-1}$) component also has a steeply voltage-dependent charge magnitude ($z \approx 1$; Fig. 4d), and a relaxation rate that increases with $[\text{Na}]_o$ at negative potentials and shows a high activation energy ($\sim 70\text{ kJ mol}^{-1}$; not shown) and, hence, probably reflects the reaction that de-occludes the second Na⁺. The fast component mirrors the time course of the distributed membrane capacitance transient and so must reflect charge transitions with rates $\geq 10^6\text{ s}^{-1}$, appropriate for rapid Na⁺ release through an access channel, but still possibly rate limited by a minor conformational change that de-occludes the final Na⁺; consistent with their high speed, these relaxations show little temperature sensitivity (not shown). In further contrast to the slow and medium-speed components, the fast charge movement has extremely weak voltage sensitivity (note simple scaling of the fast component amplitude with potential over a 160-mV range in Fig. 4c), and it is seen in virtual isolation at very low $[\text{Na}]_o$ ($\leq 25\text{ mM}$; not shown), indicating that it may reflect release of the final Na⁺ ion(s) from a relatively high-affinity site(s) on P-E₂ (see refs 8, 9, 12). Our failure to observe any comparably high-speed charge movement displaying the strong voltage sensitivity of the medium-speed and slow components, despite exploring a broad range of $[\text{Na}]_o$ and voltage, argues (see ref. 8) that there must be negligible steady-state occupancy of the narrow (high-field) access-channel conformation P-E₂(Na₂)-Na, which we propose (Fig. 4a) is ultimately responsible for those slower charge relaxations; this in turn implies that both rate constants leading away from that state (k_{-1} and k_2 in Fig. 4a) are relatively large.

The strictly sequential nature of the three charge components shown here indicates that the three Na⁺ may be released from the Na⁺/K⁺ pump in a fixed order. Ordered occlusion/de-occlusion of two K⁺ by kidney microsomal Na⁺/K⁺-ATPase¹⁴ and sequential occlusion, translocation and release of the two Ca²⁺ ions transported by the sarcoplasmic reticulum Ca²⁺-ATPase¹⁵ have been detected using isotopes and rapid filtration techniques (time resolution $\sim 10\text{ ms}$), but the far higher time resolution and sensitivity of the electrical recording methods used here permit extraction of finer molecular kinetic detail^{8,12,16}. Closer examination, using these methods, of the interactions of extracellular Na⁺ ions with their binding sites within the Na⁺/K⁺ pump will now be required to discern the precise molecular rearrangements that surround these principal charge movements in the Na⁺/K⁺ transport cycle. □

Methods

Giant axons from the squid *Loligo pealei* were voltage clamped¹⁷, internally dialysed and externally superfused at $20\text{--}22\text{ }^\circ\text{C}$ with Cl⁻-free solutions^{7,10} designed to restrict the pump to Na⁺ de-occlusion/release steps (Fig. 1). Intracellular (in mM; pH adjusted with HEPES): 80 Na-HEPES, 57 N-methyl-D-glucamine(NMG)-HEPES, 50 glycine, 50 phenylpropyltriethylammonium-sulphate, 5 dithiothreitol, 2.5 1,2-bis(2-aminophenoxy)ethane-N,N,N',N'-tetraacetic acid (BAPTA), 15 Mg-HEPES, 5 Tris-ATP, 5 phospho(enol)pyruvate tri-Na⁺-salt and 5 phospho-L-arginine mono-Na⁺-salt. Extracellular (in mM): 400 Na-isethionate, 75 Ca-sulphamate, 1 3,4-diaminopyridine, 2×10^{-4} tetrodotoxin, 5 Tris-HEPES and 0.05 EDTA (pH 7.7). Osmolality of all solutions was $\sim 930\text{ mOsmol kg}^{-1}$. To lower $[\text{Na}]_o$, Na-isethionate was replaced by tetramethylammonium-sulphamate or NMG-sulphamate. Voltage pulses were generated and currents recorded using a 16-bit PC44 A-D/D-A converter board (Innovative Technologies) with software developed in-house. Currents were filtered at 12.5–200 kHz, then sampled at 20 kHz–2 MHz. Current records were sometimes acquired after subtraction of appropriately amplified small current signals, obtained in a voltage range where pump-mediated

charge movement tended towards saturation, to minimize currents from linear membrane capacitance. Pump current was determined as current sensitive to $100\text{ }\mu\text{M H}_2\text{DTG}^{10}$.

Received 22 September; accepted 17 December 1999.

- Post, R. L., Hegyvary, C. & Kume, S. Activation by adenosine triphosphate in the phosphorylation kinetics of sodium and potassium ion transport adenosine triphosphatase. *J. Biol. Chem.* **247**, 6350–6540 (1972).
- Beaugé, L. A. & Glynn, I. M. Occlusion of K ions in the unphosphorylated sodium pump. *Nature* **280**, 510–512 (1979).
- Garrahan, P. J. & Glynn, I. M. The behaviour of the sodium pump in red cells in the absence of external potassium. *J. Physiol.* **192**, 161–174 (1967).
- Fendler, K., Grell, E., Haubs, M. & Bamberg, E. Pump currents generated by the purified Na⁺/K⁺-ATPase from kidney on black lipid membranes. *EMBO J.* **4**, 3079–3085 (1985).
- Nakao, M. & Gadsby, D. C. Voltage dependence of Na translocation by the Na/K pump. *Nature* **323**, 628–630 (1986).
- Läuger, P. *Electrogenic Ion Pumps* (Sinauer, Sunderland, MA, 1991).
- Gadsby, D. C., Rakowski, R. F. & De Weer, P. Extracellular access to the Na,K pump: pathway similar to ion channel. *Science* **260**, 100–103 (1993).
- Hilgemann, D. W. Channel-like function of the Na,K pump probed at microsecond resolution in giant membrane patches. *Science* **263**, 1429–1432 (1994).
- Heyse, S., Wuddel, I., Apell, H. J. & Sturmer, W. Partial reactions of the Na,K-ATPase: determination of rate constants. *J. Gen. Physiol.* **104**, 197–240 (1994).
- Rakowski, R. F., Gadsby, D. C. & De Weer, P. Stoichiometry and voltage-dependence of the sodium pump in voltage-clamped, internally-dialyzed squid giant axon. *J. Gen. Physiol.* **93**, 903–941 (1989).
- Läuger, P. & Apell, H. J. Transient behaviour of the Na⁺/K⁺-pump: microscopic analysis of nonstationary ion-translocation. *Biochim. Biophys. Acta* **944**, 451–464 (1988).
- Wuddel, I. & Apell, H. J. Electrogenicity of the sodium transport pathway in the Na,K-ATPase probed by charge-pulse experiments. *Biophys. J.* **69**, 909–921 (1995).
- Friedrich, T. & Nagel, G. Comparison of Na⁺/K⁺-ATPase pump currents activated by ATP concentration or voltage jumps. *Biophys. J.* **73**, 186–194 (1997).
- Forbush, B. Rapid release of 42K or 86Rb from two distinct transport sites on the Na,K-pump in the presence of Pi or vanadate. *J. Biol. Chem.* **262**, 11116–11127 (1987).
- Inesi, G. Characterization of partial reactions in the catalytic and transport cycle of sarcoplasmic reticulum ATPase. *J. Biol. Chem.* **262**, 16338–16342 (1987).
- Lu, C.-C. *et al.* Membrane transport mechanisms probed by capacitance measurements with megahertz voltage clamp. *Proc. Natl Acad. Sci. USA* **92**, 11220–11224 (1995).
- Bezanilla, F., White, M. M. & Taylor, R. E. Gating currents associated with potassium channel activation. *Nature* **296**, 657–659 (1982).

Acknowledgements

This work was supported by grants from the NIH. M.H. was supported in part by the Grass Foundation, and J.W. held a HHMI Postdoctoral Research Fellowship for Physicians.

Correspondence and requests for materials should be addressed to D.C.G.

(e-mail: gadsby@rockvax.rockefeller.edu), or to M.H.

(e-mail: miguel_holmgren@hms.harvard.edu).

The 21-nucleotide *let-7* RNA regulates developmental timing in *Caenorhabditis elegans*

Brenda J. Reinhart[†], Frank J. Slack[†], Michael Basson[‡], Amy E. Pasquinelli^{*}, Jill C. Bettinger[‡], Ann E. Rougvie[#], H. Robert Horvitz[§] & Gary Ruvkun^{*}

^{*} Department of Molecular Biology, Massachusetts General Hospital, and Department of Genetics, Harvard Medical School, Boston, Massachusetts 02114, USA

[§] Howard Hughes Medical Institute, Department of Biology, Massachusetts Institute of Technology, Cambridge, Massachusetts 02139, USA

[#] Department of Genetics, Cell Biology and Development, University of Minnesota, St Paul, Minnesota 55108, USA

[†] These authors contributed equally to this work

The *C. elegans* heterochronic gene pathway consists of a cascade of regulatory genes that are temporally controlled to specify the timing of developmental events¹. Mutations in heterochronic genes cause temporal transformations in cell fates in which stage-specific events are omitted or reiterated². Here we show

[‡] Present addresses: Axys Pharmaceuticals, South San Francisco, California 94080, USA (M.B.); Ernest Gallo Clinic and Research Center, UCSF, Emeryville, California 94608, USA (J.C.B.); Department of MCDB, Yale University, New Haven CT 06520, USA (F.J.S.).